Combining Detailed Experiments, PolyUMod®, Kornucopia®, and Abaqus® to Create Accurate FE Scratch Simulations

Ted Diehl[1], Jorgen S. Bergstrom[2], Xiaohu Liu[2], Li Lin[1], Ye Zhu[1], John J. Podhiny[1], Richard T. Chou[1], and Jeffrey A. Chambers[1]

[1] DuPont, Wilmington, DE, USA, Ted.Diehl@USA.DuPont.com
[2]Veryst Engineering, LLC, Needham Heights, MA, USA, jbergstrom@veryst.com

Abstract: Creating a viable simulation approach capable of representing key fundamental aspects of scratch of polymers is an extremely challenging task. The simulation must include complicated material response, such as nonlinear viscoelastic/viscoplastic behavior of the polymeric material at large strains. In addition, the model must include a sufficiently detailed representation of the scratching event using frictional contact between the indenter and the sample, and the model must take into account the indenter loading history. And perhaps the most challenging of all, the simulation must properly and efficiently represent the long recovery time after the scratching event during which the highly deformed polymer can partially recover. This paper discusses how Abaqus/Explicit models using the PolyUMod® advanced Parallel Network Material models were used in conjunction with detail experiments processed by Kornucopia® to create scratch simulations that correlated well to several physical scratch tests. In particular, various technical challenges that were solved during the development of a successful modeling strategy are described and discussed in detail.

Keywords: Constitutive Model, Creep, Damage, Experimental Verification, Plasticity, Polymer, Post-Processing, Viscoelasticity, Viscoplasticity, Material Model calibration, User-Material Model, Nonlinear Analysis, Large Deformation, Remapping, Data Smoothing, Data Filtering.

1. Introduction

Generating a predictive finite element (FE) simulation for polymers being scratched by comparatively rigid indenters is difficult because it requires more than just a good FE model. At a minimum, the following entities are needed: 1) A sufficiently accurate polymer constitutive model capable of capturing very large strain, inelastic deformation, and rate/time dependence, 2) Advanced material experiments that generate sufficient data to calibrate the parameters of the material law, 3) Robust FEA methods that can incorporate the advanced material model, support sliding contact, and can handle extremely large strains which will cause severe element distortions, 4) Detailed polymer scratch experiments with 3-D surface imaging technology to capture the scratched profile for comparison to the FEA simulations, and 5) A method to manipulate a large amount of non-ideal, messy data (from both the experiments and simulations).

This paper describes several details and various key aspects of the required technology listed above, all applied to producing validated scratch simulations of polymers.

2. Material Characterization

To investigate and develop a sufficient approach, three polymeric materials were studied. Two of the polymers were grades of DuPont Surlyn® (an ethylene copolymer ionomer), namely Surlyn® 9950 and a Surlyn® blend of grades 1706/1707. These two materials are differentiated from each other by such factors as their percent neutralization, acid content and other formulation make-up. The third material was PMMA, a polymethylmethacrylate. PMMA is noticeably different – stiffer and harder – than the Surlyn® materials. Also, PMMA is based on the molecule methyl methacrylate and is not an ethylene copolymer ionomer.

During a scratch event, each of the polymers is loaded in a highly complex, multi-axial state of deformation. If the indenter load is large enough, the polymer will experience inelastic deformation, potentially to very severe levels, including even local failure and cracking in some instances.[1] Because of the viscoplastic nature of the polymers, their response in a scratch event will also be time-dependent, both in terms of the indenter's applied deformation rate and in terms of recovery time of the scratched polymer after the intender is no longer interacting with the specimen.

The above conditions suggest that material characterization tests need to sufficiently exercise the material in terms of time, strain, and stress. Ideally, such tests would be carried out using several deformation modes (compression, tension, shear, uniaxial, biaxial, etc.) over a range of strain levels and strain rates, and with some tests including loading followed by unloading. It would also be beneficial to have some of the tests measure longer-term relaxation behavior, as this is an important aspect of the polymer materials' self-healing response after the scratch event has occurred.

As this paper documents an initial investigation of scratch simulation, most of the material testing was limited to a single, advanced test design – uniaxial puck-compression using a Ziggurat protocol. Figure 1 depicts an idealized version of the test showing how it exercises the material as a function of time and strain, including large strains causing inelastic deformation. The test is dominated by compression, but also induces a complex and varying multi-axial strain state throughout the sample because the puck will non-uniformly bulge due to the frictional boundary conditions of the plates that compress the puck. The addition of Ziggurat shear and Ziggurat tension tests would further improve material characterization, and they will be utilized in a later phase of this work (not reported here). The Ziggurat protocol, given its name from the visual appearance of the applied strain vs. time curve, combines a traditional cyclic load/unload protocol with constant strain holds over various times during the test to measure relaxation behavior. When combined with a nonlinear optimization algorithm for material law calibration, this type of testing protocol produces a very effective approach.

2.1 Experimental Data

Figure 2 presents some of the Ziggurat puck compression test data measured for the Surlyn® 1706/1707 blend material. The measures of stress and strain plotted are engineering (often termed

[1] In the present work, failure and cracking was not included in the FE modeling efforts. There were some instances where cracks appeared in the scratch data from physical experiments.

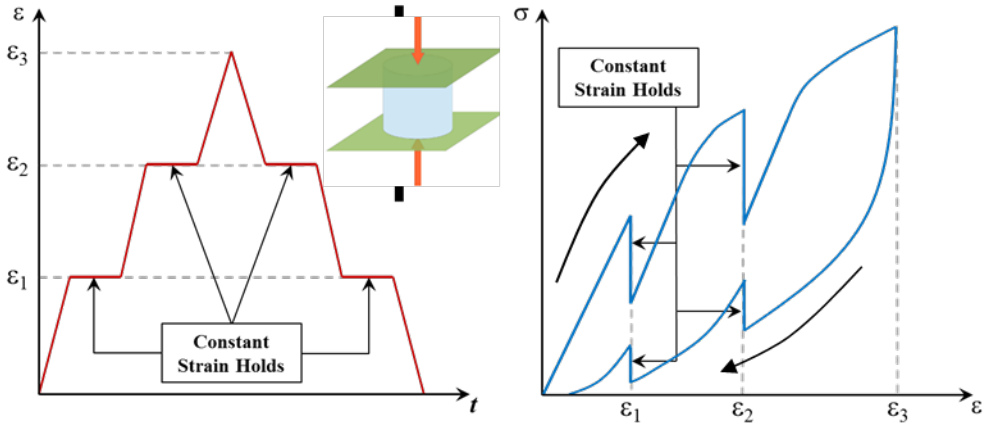

Figure 1: Idealization of a compression Ziggurat test depicting the imposed strain vs. time boundary condition and the resulting stress vs. strain response of the sample.

as *nominal*) measures based on the sample's undeformed geometry. Specifically, the stress is defined as the applied compression load divided by the sample's undeformed cross-section and the strain is defined as the change in height of the sample divided by its undeformed height. The measures are *apparent* in the sense that actual strains (and stresses) in the sample vary through-out the sample because of the non-ideal boundary conditions that occur due to the frictional contact between the sample and the steel platens.

The measurement of apparent strain in the test was done in two different ways, one based on displacements derived from the load-frame's crosshead motion, and one based on the average of three laser displacement gages that measured motion of the platens. The crosshead motion data contains deformation of the sample (desirable) as well as deformations of the load train and fixtures (undesirable). Due to the nature of the equipment used in the testing, the crosshead motion was needed to control the system. The laser gage data, which is not distorted by the fixture compliance (load train and fixtures combined), is used to measure the sample's apparent strain. Three gages mounted 120 degrees apart around the specimen are used to confirm that undesirable tilting of the platens is sufficiently small as to be negligible. Figure 2a and Figure 2b show how the resulting stress-strain data differs based on which measure of strain, crosshead or laser gage, is utilized. This is most evident in the various "strain-hold" stages where the crosshead motion was held constant, but the laser gages recorded that the sample strain continued to vary slightly overtime. This is because as the sample relaxed during those segments of the test, its stress and thus its load reduced, which in turn put less load on the compliant test fixtures and caused their length to change slightly, allowing further dimension changes (strain) in the sample. The influence of the fixture compliance is also seen in the maximum strain applied, where the laser gage measurements recorded 17% less strain than the crosshead measurements.

Figure 2c shows how both the laser-based strain and stress varied over time in the test. The sample's strain vs. time profile is noticeably different from the idealized Ziggurat profile presented

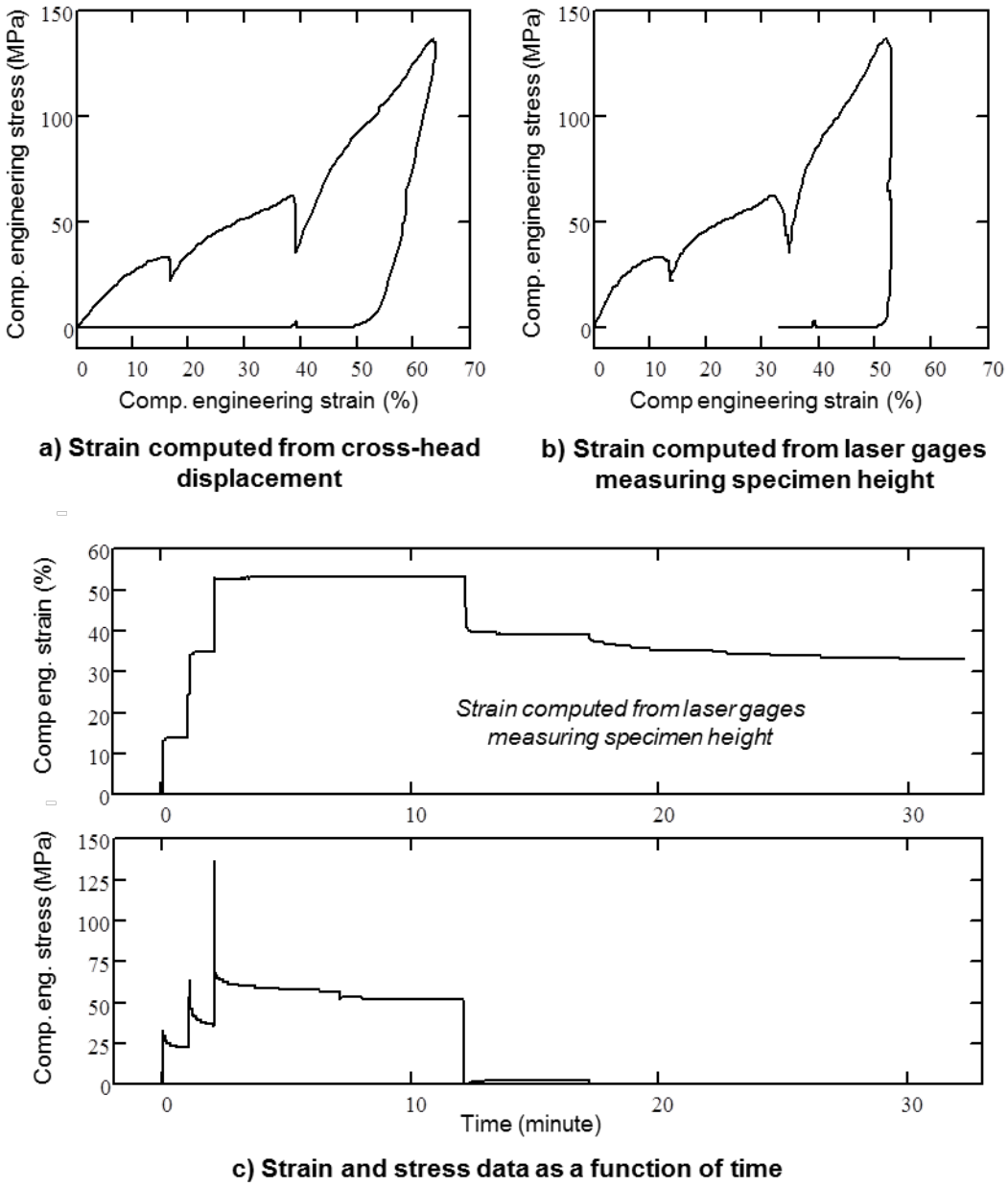

Figure 2: Ziggurat puck compression test data for Surlyn® 1706/1707 blend. Plot depicts measurement data after being processed by Kornucopia®. Both stress and strain data are apparent measures. The applied apparent strain rate was 0.1 s^{-1}.

in Figure 1. This is caused by several factors: 1) The nature of the response of the Surlyn® material tested required a non-symmetric Ziggurat profile to ensure relaxation holds occurred appropriately during both loading and unloading stages, and 2) the large relaxation time constant of the material required the constant strain hold times to be quite long (measured in minutes) relative to the loading and unloading segments (measured in seconds).

A few other comments on the test data are important. The raw version of the measured data (not shown) contained over 35,000 points, non-uniformly spaced in time. The data also had a small amount of noise in it from the laser gages and had some start-up distortions in the initial small-strain regime due to small geometry irregularities in the samples tested. To improve material calibration and make the process efficient, the raw data was pre-processed using Kornucopia® (www.BodieTech.com). In doing so, a worksheet was created to segment each test into various load (or unload) segments and constant strain hold segments, via a semi-automatic approach powered by Kornucopia® functionality. With the data segmented, it was then smoothed and resampled so that each load/unload segment had approximately 100 equally spaced points and each constant-strain hold segment had 100 logarithmically spaced points. Additionally, the distortion at the beginning of the test was trimmed and corrected with a linear extrapolation technique. This data processing significantly improved the data quality and reduced the dataset to less than 1,000 points, improving the numerical efficiency of the material model calibration step (to be described in the next section).

The data presented in Figure 2 was measured using an applied crosshead strain rate of 0.1 s^{-1}. Other test data, not shown for brevity but used to calibrate the material model, included a much slower strain rate of 0.005 s^{-1}. Similar overall testing protocols were followed for the other two polymer materials in the study.

2.2 Material Constitutive Model and Its Calibration

The experimental data summarized in the previous section clearly show that the materials studied exhibit a non-linear viscoplastic response characterized by significant flow and partial recovery after unloading. These characteristics can be accurately captured using the Three Network Model (TNM) from the PolyUMod library of user-material models for Abaqus (www.veryst.com). The TNM is an advanced material model that has been shown to capture the response of many different thermoplastic materials (Bergstrom, 2010). Figure 3 shows the rheological structure of the TNM.

The details of the governing equations for the TNM can be found in references (Bergstrom, 2010, and the PolyUMod documentation). In short, the stress response of each of the three networks is given by the hyperelastic Arruda-Boyce eight-chain model (Arruda, 1993). The stiffness of network B is taken to evolve with the plastic strain accumulation in Network A. The total stress is given by the sum of the Cauchy stress tensor in each network. The rate of viscoplastic flow of Networks A and B is given by a power law expression of the driving deviatoric shear stress and temperature, and the flow resistance is taken to be pressure dependent. Note that this material model exhibits true plasticity despite the presence of the Network C component. The cause of the plasticity is the energy barrier for flow that is inherent in the flow equations.

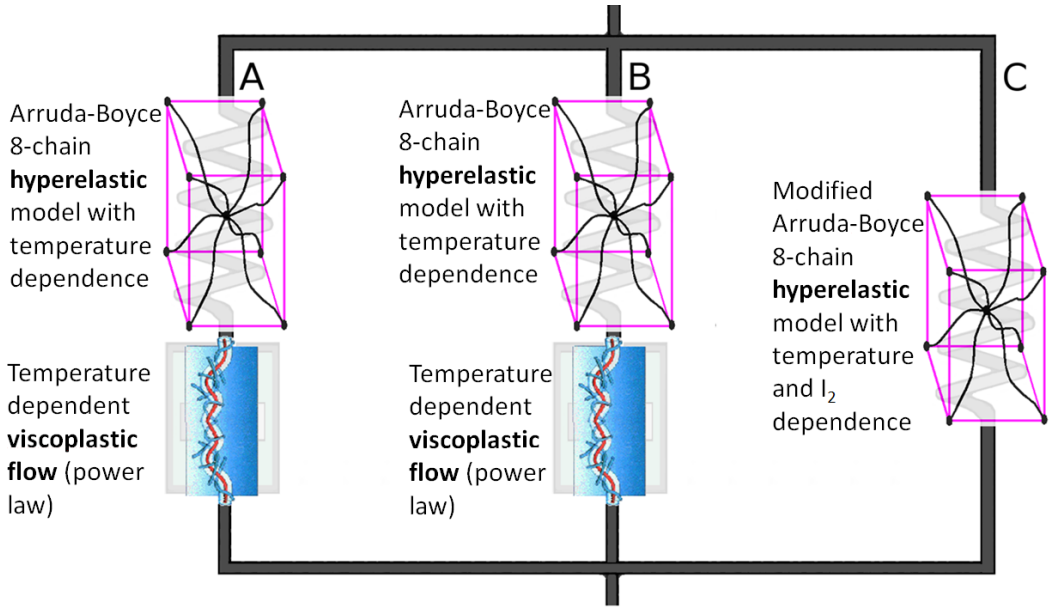

Figure 3: The Three Network Model (TNM) can be represented using a rheological approach with non-linear springs and dashpots.

The material model was calibrated to the experimental data using the MCalibration® software (www.veryst.com). The calibration was performed using the following steps:

1. Read in the experimental data from all tests into the MCalibration® software.
2. Assign each experimental data set as a "Compression with Friction" load case, see Figure 4. This load case automatically creates an Abaqus FE model of the experimental test setup and boundary conditions (including friction). This is important so as to get a model that most closely represents the configuration of the experimental test that drives the calibration procedure.
3. Select the Three Network Model.
4. Start the automatic material model calibration.

The material model calibration stops once it has found an optimal set of material model parameters. Figure 5 shows a MCalibration screen shot of the calibration of Surlyn® 1706/1707 blend. The calibrated material model was then exported to Abaqus/CAE. Figure 5 shows that the calibrated material model captures the strain-rate dependent yield stress, non-linear hardening response, and the recovery response after unloading. Figure 6 depicts all three materials showing their behavior during the 0.005 s^{-1} tests and the resulting PolyUMod fits.

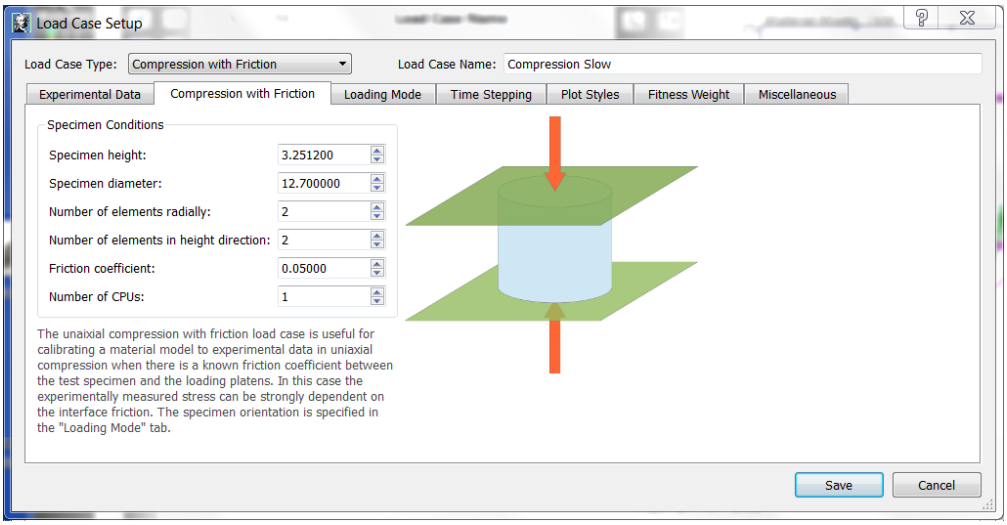

Figure 4: The experimental data files were represented using the "Compression with Friction" load case that is available in MCalibration.

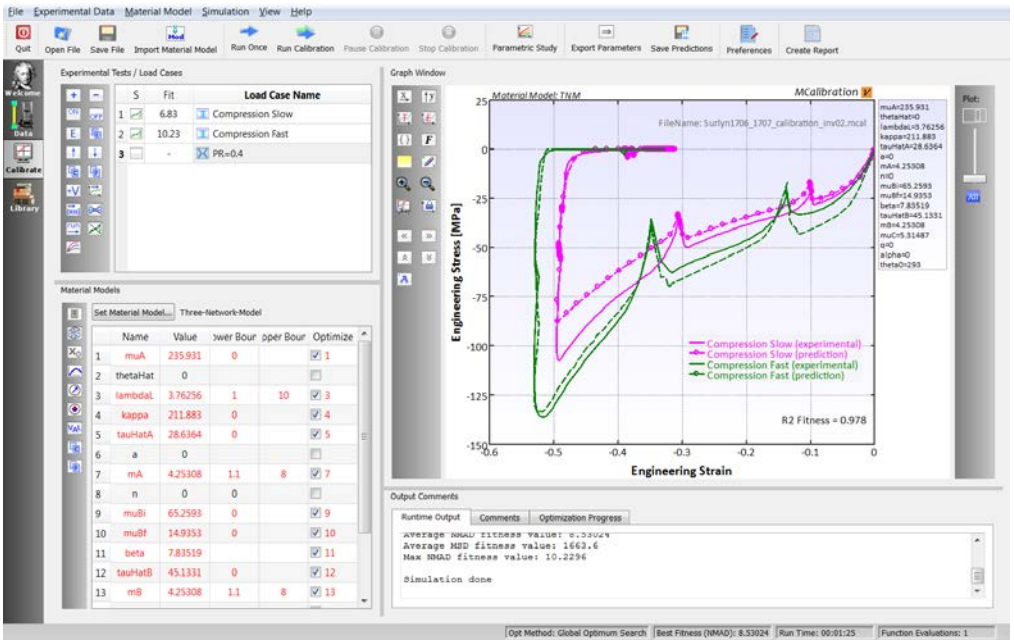

Figure 5: Screen shot of MCalibration at the end of the material model calibration of Surlyn® 1706/1707.

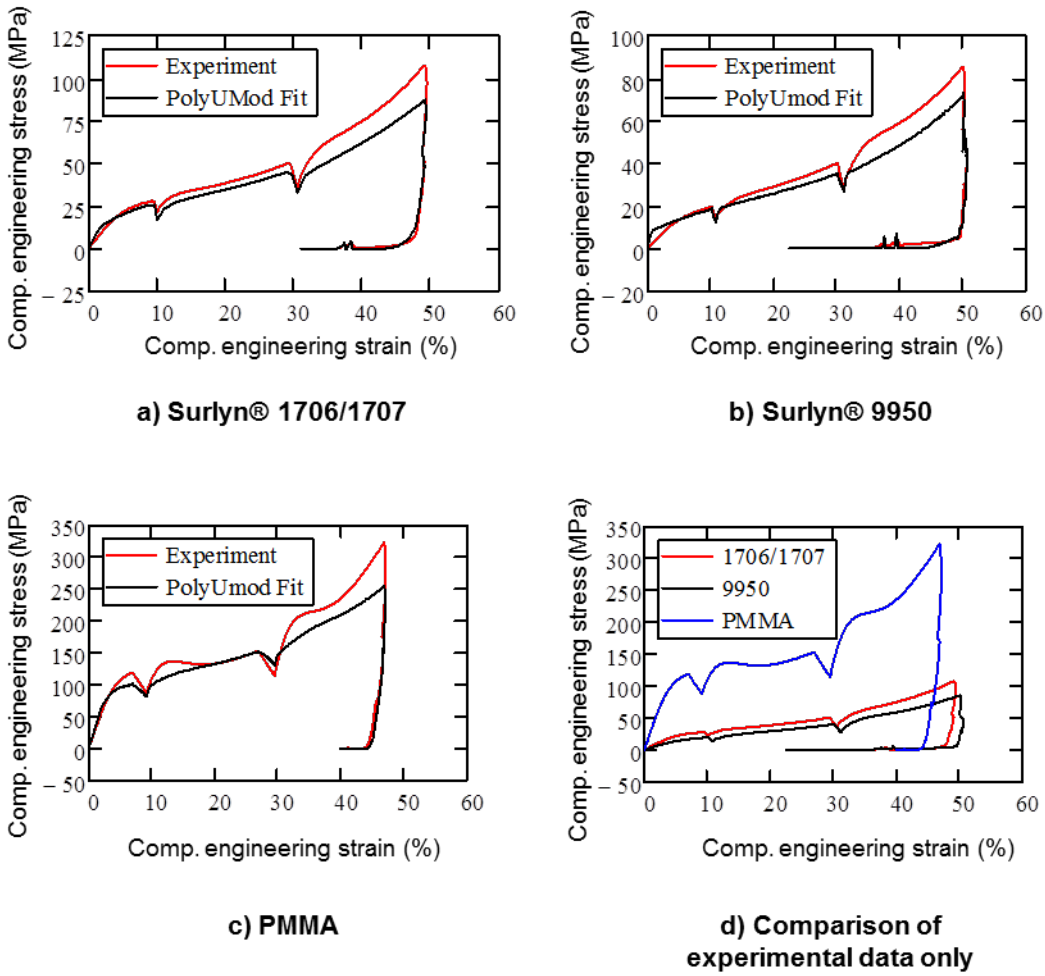

Figure 6: Summary of material test data for three polymers studied and their PolyUMod® fits. This figure shows only evaluation of a low strain rate of 0.005 s^{-1}. The PolyUMod® calibration actually used both the low strain rate data (shown) and high strain rate data (not shown for brevity) in the nonlinear calibration procedure.

3. Finite Element Simulation Approach

The experimental scratch tests were simulated using Abaqus/Explicit with the calibrated material models from the previous section. In these simulations a 100 micron radius scratch tip was

modeled using a rigid surface, and the polymer test specimen was divided into two regions: a coarse region (500 C3D8R elements), and a fine region (55,000 C3D8R elements). The fine mesh region was adaptively remeshed by the solver during the solution, and the meshes in the two regions were tied together. Figure 7 shows a side view of the mesh that was used in the simulations.

The scratch simulations were performed in three steps, see Figure 8. For the case of Surlyn® 1706/1707 blend, the following loading parameters were utilized. In the first step the indenter was pushed vertically down into the material a distance of 60 μm in 0.05 sec. In the second step the indenter was moved horizontally a distance of 0.6 mm in 0.15 sec. In the final step the indenter was unloaded by moving it vertically upward a distance of 66 μm in 0.05 sec. (Scratch depth was 13.5 μm for PMMA and 70 μm for Surlyn® 9950; all other loading parameters were the same as described above.) It is also noted that the simulations were performed in displacement control (making the Explicit solution easier to control), whereas the experiments were performed in load control. For the entire solution, the friction coefficient between the indenter and the polymer test specimen was 0.4 (taken from experimental data).

An important physical phenomenon that needed to be represented in the model was the creep recovery that occurs in the material after it is scratched. This means that over time, scratched polymers undergo self-healing or recovery. This behavior, however, occurs over a long time period, measured in minutes, hours, or even days, depending on the nature of viscoplasticity in the

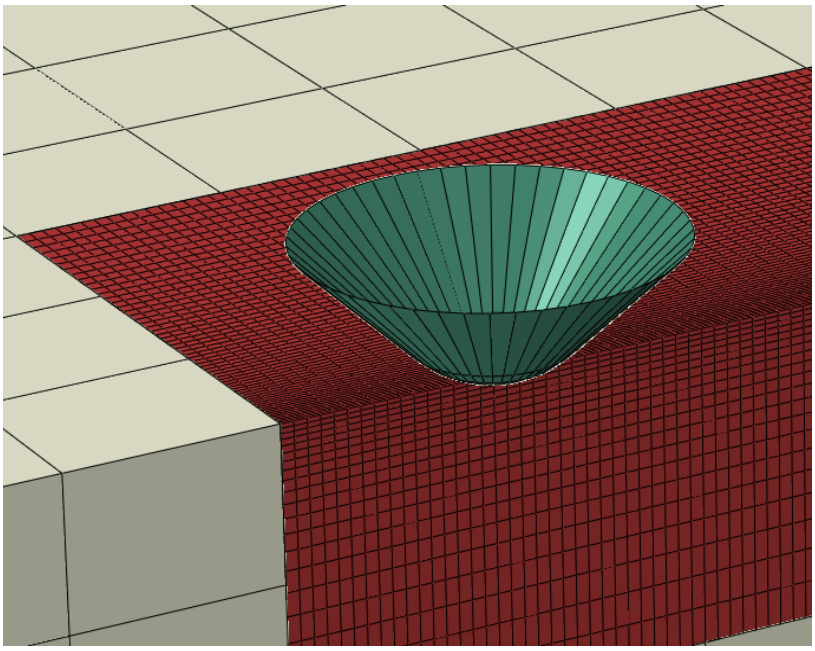

Figure 7: Finite element mesh used to represent a 100 micron tip indenter scratching a polymer surface. The model is using half symmetry.

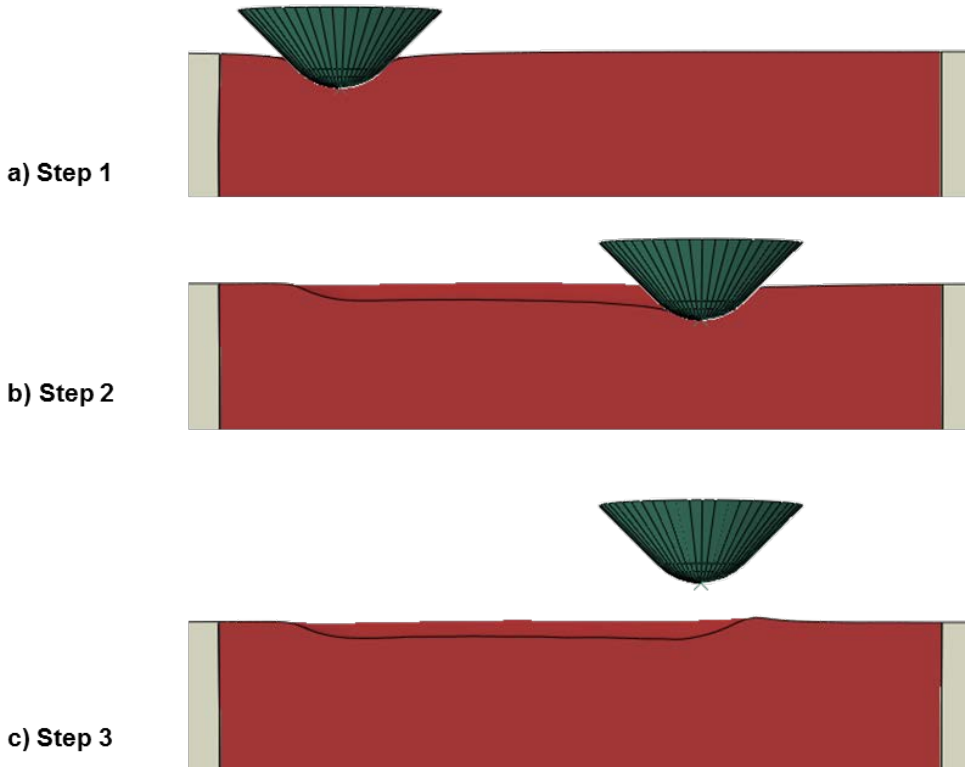

Figure 8: The scratch simulations were performed in 3 steps: (1) Push the indenter down into the material, (2) scratch the surface by moving the indenter horizontally, (3) unload the indenter and let the material relax.

material. To keep the explicit dynamics simulation computationally viable, a technique of gradually increasing mass scaling, in stages, was used in the final relaxation step of the simulation. This enabled a relatively long simulation time in the explicit FE computation to be achieved, although as shown in Figure 9, the results were not ideal. Figure 9 presents data from a scratch simulation of Surlyn® 1706/1707, results for Surlyn® 9950 and PMMA (not shown) was similar in nature. Figure 9a shows the motion as computed of a node on the surface of the polymer in the path of the scratch. Figure 9b shows the same data, zoomed to 4 sec of total time, clearly indicating the three stages. This data shows significant dynamic vibrations that was caused by changing the mass scaling at each stage. The solutions depicted included mass-proportional Rayleigh damping in an effort to damp out oscillations. Figure 9c shows the same data with each stage separately regularized and smoothed using a DSP-based lowpass filter with an advanced

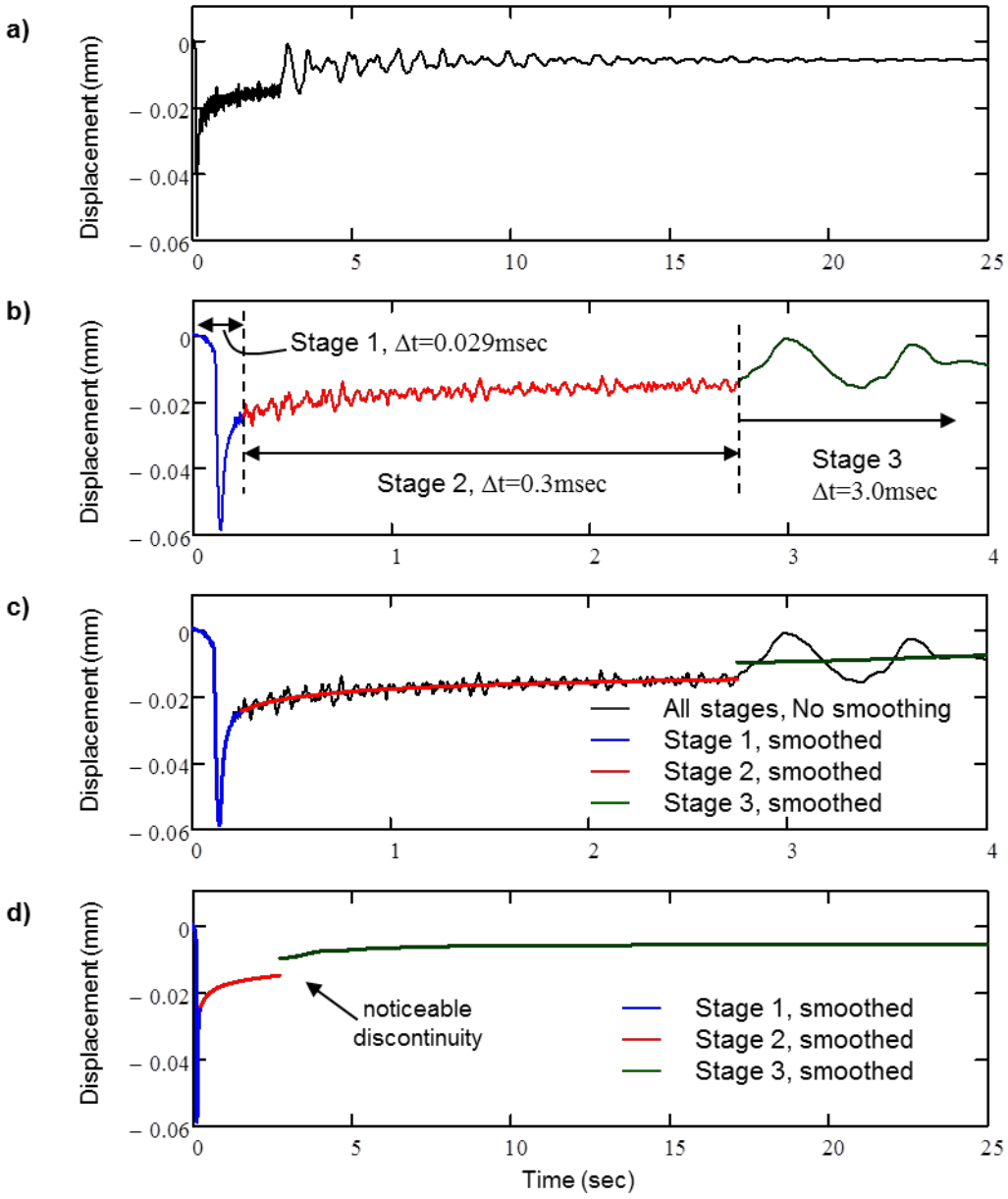

Figure 9: Assessment of the influence of using three different stages of mass scaling to speed up solution. Data shown is for a scratch simulation of Surlyn® 1706/1707. The data shows the creep recovery of a single node on the polymer's surface along the scratch path.

end-assumption prediction algorithm from Kornucopia®. Figure 9d presents only the smoothed results which clearly show modest discontinuities in the solution caused by changing mass scaling. These initial results show that the approach is promising, but clearly more investigation needs to be done to fine-tune the methodology.

4. Correlation of Scratch Simulations and Scratch Experiments

The next two subsections describe the scratch experiments performed, the method of 3-D surface profiling used to characterize them, and how the FEA models from the previous section correlated to the physical scratch results. It is noted that the physical scratch tests used a horizontal motion of 0.5 mm/min which is notably slower than the loading rate of 240.0 mm/min used in the FEA models. This inconsistency in loading rate will cause the FEA model to over-predict the resisting force under scratch. But with displacement control, it has a smaller influence on the main focus of this study which is the scratch profile after relaxation. This being said, future studies are planned to achieve a more realistic loading rate in FEA simulations.

4.1 Scratch experiments

In the complete study, scratch experiments of progressive and step function loading were performed using a nano-scratch tester and a macro-scratch tester from CSM Instruments. Indenters used are 90 degree conical shapes with spherical radius of 2, 20, and 100 micrometers. However, only scratch results of step loading with 100 micrometers tip are reported here.

Figure 10 presents a selective summary of some of the scratch data collected and processed in the study. During the scratch experiments, a specified vertical indenter force is applied and as the indenter moves horizontal per a prescribed speed while the indenter's vertical motion is recorded. Approximately 24 hours after a scratch is completed, the sample geometry is scanned using a Zygo 3-D Optical Surface Profiler. The 24 hour delay in scanning the profile allows the material time to partially self-heal the scratch due to the viscoplastic nature of the polymer. Using 3-D surface profiles of the scratch offers the possibility of a much richer dataset to validate FE models against. However, as seen in Figure 10a, the experimentally measured profiles had large amounts of irregular drop-outs and noise. Figure 10b shows the same measured data after it was healed with functionality available in Kornucopia® and Mathcad®. Figure 10c shows a different polymer scratch dataset after it was processed by Kornucopia®, including the contraction of its complicated 3-D surface profile down to aligned 2-D cross-sections, including the averaging of the various curves to a single cross-section and the identification of 9 key points in the cross-section.

4.2 Correlation of FE models and experiments

All scratch experiments performed on the three polymers were processed in the manner described in Section 4.1. To compare FE models of the three polymers, a similar post- processing procedure was used, but with a few differences. The FE data had no missing values (drop-outs) as was the case with the experimental data. However, the fact that the FE model used adaptive meshing made it impossible to directly compare the FE data to the experiments since the "scanning grid" of the FE data surface was not rectangular like the experimental data. This was easily remedied by remapping the FE results using functionality available in Kornucopia® and Mathcad®.

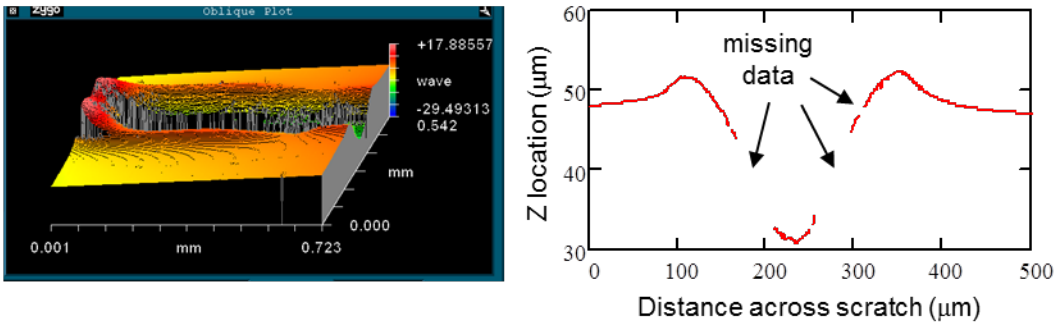

a) Raw Zygo measurement of Surlyn® 9950, scratched with a 1,500mN load

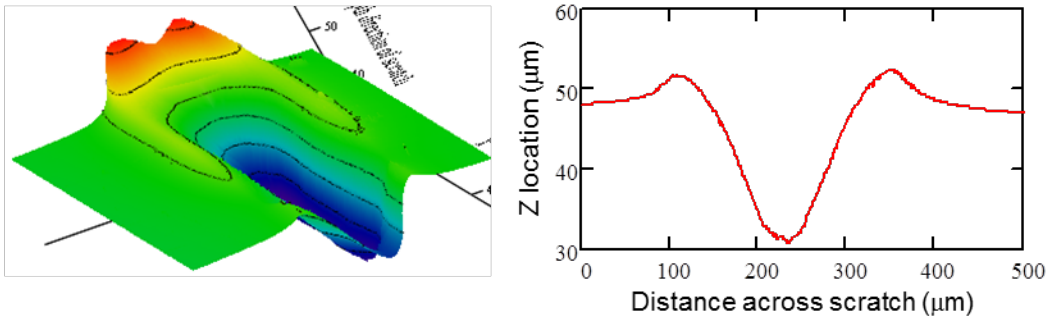

b) Above data after healing with Kornucopia® and Mathcad®.

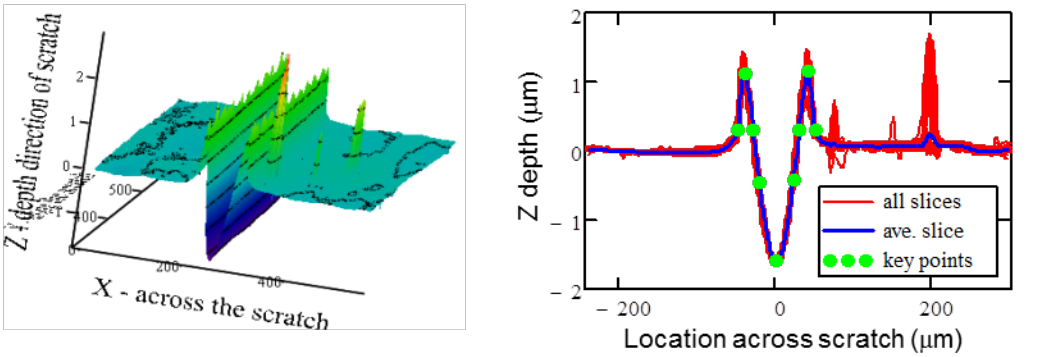

c) Healed PMMA data (1,000mN scratch load) with additional Kornucopia® processing

Figure 10: Depiction of several key steps in the processing of raw experimental scratch data, ultimately resulting in an average cross-section characterization of the 3-D scratch.

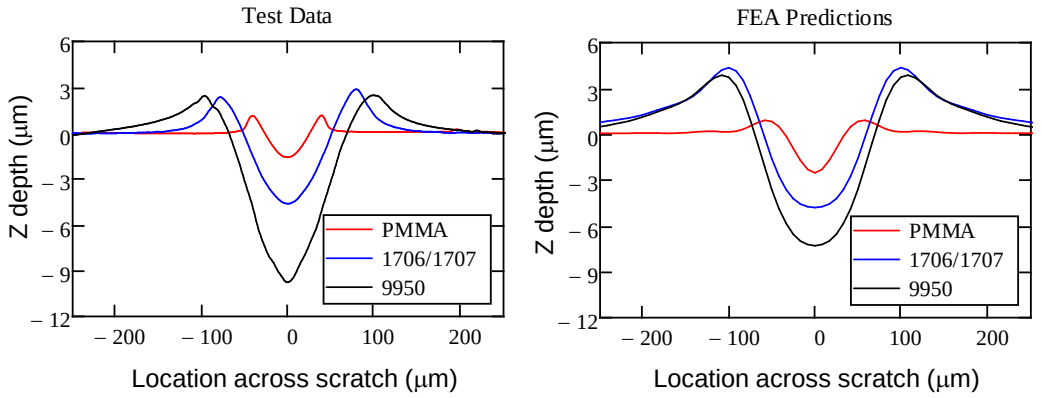

Figure 11: Correlation of models and physical tests for the scratch cross sections of three different materials.

With the FE data processed in a consistent manner to the experimental scratch data, the final validation assessments of the entire modeling approach could be completed. Figure 11 presents the final average 2-D scratch profiles measured from physical tests and calculated from the Abaqus models using the PolyUMod® Three Network (material) Models. The two sets of graphs are scaled identically to make correlation assessments easier. The results show that the FE models predict a similar ordering of the polymer materials relative to their scratch response. The match between the models and physical testing is not perfect, but given the complexity of the phenomenon being simulated, these results are considered to be very encouraging.

Some possible causes for discrepancies between the FE models and the physical tests include:

1. Constitutive law fitting or form – the results depicted from Figure 6 show that the model did a good job in representing the material data, but it was not perfect. Further investigations could be performed to determine if a better fit can be achieved during the nonlinear optimization process used during parameter calibration, or if a different constitutive representation would improve material representation. It is also possible that the MCalibration material model curve fits (and hence the material representation) will be improved by including additional material test data in different loading modes (namely shear and uniaxial tension).
2. A more refined FE mesh. The FE scratch model results appear slightly more rounded as compared to the actual tests. This is possibly a result of the mesh size used in the analysis which was chosen to strike a balance between solution effort and accuracy.
3. Some of the materials show evidence of cracks in the scratched profiles from physical testing, a behavior that was not included in the current modeling approach. Including the

ability to simulate failure and cracking would be extremely challenging, but may lead to improved correlations if such modeling can be done.

4. The time-segmented mass scaling approach used in the FE model appears to require further investigation (perhaps additional fine tuning in the way it was utilized).

5. Conclusions

This study has demonstrated how detailed experiments combined with advanced FE modeling approaches and pre/post data analysis methods have been combined to create viable scratch simulations of polymeric materials. The methodology was developed and demonstrated using three different polymeric materials, two DuPont Surlyn® grades and PMMA. The FE simulations were carried out using Abaqus/Explicit, employing several techniques including mass scaling and adaptive re-meshing. The nonlinear viscoplastic behavior of the polymers was successfully represented using the PolyUMod® Three Network (material) Model. Each of the three polymer's material models were calibrated via MCalibration® software using test data derived from Ziggurat puck-compression tests. All the test data, both the material testing and the scratch validation testing, along with the Abaqus FE simulation results data, was processed by Kornucopia® to improve data interpretations and expedite the processing of large amounts of data.

Combining the various software tools, testing protocols, and simulation and data analysis techniques, the study has demonstrated that accurate scratch simulations of polymeric materials are possible.

6. References

1. Abaqus Users Manual, Version 6.10-1, Dassault Systémes Simulia Corp., Providence, RI.

2. Arruda, E. M. and Boyce, M. C., "A three-dimensional constitutive model for the large stretch behavior of rubber elastic materials", J. Mech. Phys. Solids.41, 2, pp. 389–412, 1993.

3. Bergstrom, J. S. and Bischoff., J. E., "An Advanced Thermomechanical Constitutive Model for UHMWPE," *Int. J. Structural Changes in Solids*, Vol 2, No 1, pp. 31-39, 2010.

4. Kornucopia® v1.6, 2012, available from Bodie Technology, Inc., www.BodieTech.com .

5. MCalibration® v2.2.2, 2013, available from Veryst Engineering, LCC, www.veryst.com.

6. PolyUMod® library of user-material models for Abaqus, v2.2.2, 2013, available from Veryst Engineering, LLC, www.veryst.com .

7. Acknowledgements

The authors greatly appreciate the support and funding of M. Shawn McCutchen, Global ECP Technology Manager, Packaging & Industrial Polymers, DuPont. We also thank Jing Li and Ben Foltz, DuPont's Corporate Center for Analytical Science, for performing the scratch tests and their 3-D images.